Acta Sci. Pol.
Formatio Circumiectus 23 (4) 2024, 99–111
ENVIRONMENTAL PROCESSES

www.acta.urk.edu.pl ISSN 1644-0765 DOI: http://dx.doi.org/10.15576/ASP.FC/196937

ORIGINAL PAPER Accepted: 6.12.2024

INFLUENCE OF GEOMETRIC DOMAIN ON HYDRODYNAMIC MODELING AT ESTUARY BOUNDARIES

Edgar Ulises Coronel-Quezada[1] 0009-0007-6220-1923,
Fabian Rivera-Trejo[1]✉ 0000-0002-6722-0863,
Gaston Priego-Hernandez[2] 0000-0003-2236-9426,
Alejandro Mendoza-Resendiz[3] 0000-0002-2479-9799

[1] Engineering and Architecture División, Juarez Autonomous University of Tabasco, Tabasco, Mexico
[2] Basic Sciences Division, Juarez Autonomous University of Tabasco, Tabasco, Mexico
[3] Institute of Engineering, National Autonomous University of Mexico, Coyoacan, Mexico

ABSTRACT

Aim of the study

Numerical modeling of estuaries is a complex task due to the effect of the tide and its interaction between the estuary outlet and the sea. Therefore, the following question arises: Does the length and shape of the geometric domain at the downstream boundary of an estuary (interaction lagoon-mar) affect its hydrodynamic modeling?

Material and methods

Two-dimensional (2D) numerical simulations were performed using HEC-RAS V6.3.1. Input data included a high-resolution digital model, a bathymetric survey of the study area, tidal data, and a field measurement campaign. Five geometric domains were tested as downstream boundary conditions: rectangular; large semi-circular; medium semi-circular; small semi-circular; and a cross-section. Additionally, two types (versions) of the solution equations were tested: simplified, considering only the diffusion terms, and with the full equations.

Results and conclusions

Two profiles were selected to analyze the results: longitudinal and transversal over the estuary outlet (lagoon-sea interconnection channel). The water surface levels, hydraulic slope, and velocities were compared. We found little significant difference in the offshore-dominated conditions but a considerable difference in the cross-sectional condition. Also, as expected, significant differences were found when using the full versus simplified equations.

Keywords: HEC-RAS, boundary conditions, numerical simulation, field measurements

INTRODUCTION

Estuaries are unique and vital ecosystems formed at the mouths of rivers, where freshwater meets saltwater from the sea. These sites are of great ecological and socio-economic importance, as they host significant biodiversity and play crucial role in balancing the coastal ecosystems (Shan et al., 2013). In addition to creating a habitat conducive to a wide range of species, including fish, birds, crustaceans, and aquatic

✉e-mail: jgfabianrivera@gmail.com

plants, they also provide a habitat for a wide range of species, including fish, birds, crustaceans, and aquatic plants (Clunies et al. 2017; de Haas et al. 2018), and act as natural nurseries for many marine species, providing shelter and food during their initial stages of life. Economically, they are essential, as human communities depend on them. Activities such as commercial and recreational fishing, tourism, and aquaculture farms are carried out in these areas (Ballester and Castro, 2016), contributing significantly to the local economy. Tides cause the water to flow in both directions (Seabergh, 2008; Douglass and Webb, 2020), giving rise to a natural flushing that maintains good water quality and reasonable salinity levels. Therefore, knowing and predicting these flow exchanges is essential to preserve this delicate ecological balance, even more so when human activities exist in these areas (Kennish, 2002).

HEC-RAS V.6.3.5 software was used in this research (Brunner, 2021). It was selected from among all of the available tools because it offers open access, and it has the processing capacity for estuarine systems (Bakhtyar et al., 2020; Diedhiou et al., 2020; Nizar et al., 2022); also, it has been validated and recognized worldwide (Manina et al., 2020; Namara et al., 2021; Hernandez-Ramon et al., 2023). In addition, it employs numerical methods based on the conservation laws and equations of motion of fluids. This feature allows for detailed analysis of the complex interactions between variables such as tides (Keong and Yusoff, 2022), floods (Ongdas et al., 2020), wind influences (Peng and Liu, 2019), channel morphology, and other factors that influence estuarine dynamics (Ji, 2008).

The accuracy of representing physical phenomena depends on the appropriate selection of the computational domain (Sedigh et al., 2016). The domain must balance accuracy with computational efficiency to ensure a representative and feasible simulation. We have analyzed five computational domains by varying their shape and length using topography and bathymetry data, starting with a whole domain based on field surveys. Our goal was to answer three questions: 1) Do different geometric domains affect the estuary-sea hydrodynamics? 2) Which domain performs best? 3) Which is the least favorable? Using an estuary in Tabasco, Mexico, as a case study, we compared the results against field measurements. We also examined the impact of using simplified versus full equations in HEC-RAS on the hydrodynamic analysis.

STUDY AREA

The Carmen-Pajonal-Machona lagoon system is located in Sánchez Magallanes, Tabasco, Mexico (Figure 1), with UTM coordinates: 437578.97, 2033383.19, zone 15N, ITRF92 datum. It is used for shellfish and shrimp farming, requiring constant water recirculation. The lagoon receives freshwater from the Santana River. It connects to the sea via an artificial channel built in 1975. However, a sediment bar forms annually at this outlet, necessitating frequent dredging.

METHODOLOGY

The initial parameters used were field measurements obtained in 2016 by Ballester and Castro (2016). During this campaign, velocity values were recorded with an Acoustic Doppler Current Profiler (Priego-Hernández et al., 2019). Offshore zone and the artificial channel zone have velocities in the following ranges: offshore, between 0.1 and 0.4 m · s^{-1}; in the channel, from 0.05 to 0.55 m · s^{-1}. These measurements were used to calibrate the numerical simulations in agreement with the methodology proposed by Soto-Cortes et al. (2022).

NUMERICAL MODELING

Modeling the hydrodynamic processes of an estuary using HEC-RAS allows for better management decision-making by providing information on levels and velocities in the study area, which helps to understand the health of ecosystems and to plan sustainable development strategies. In the specific case of HEC-RAS, it uses the continuity equation (Eq. 1):

$$\frac{\Omega_i^{n+1} - \Omega_i^n}{\Delta t} + \sum\nolimits_{k \in K(i)} s_{i,k} u_{N,k}^{n+\theta} \ A_k = Q_i \qquad (1)$$

where Ω is the volume of the cells (m^3), Δt is the step time (s), $s_{i,k}$ is the sign in the outward direction on the

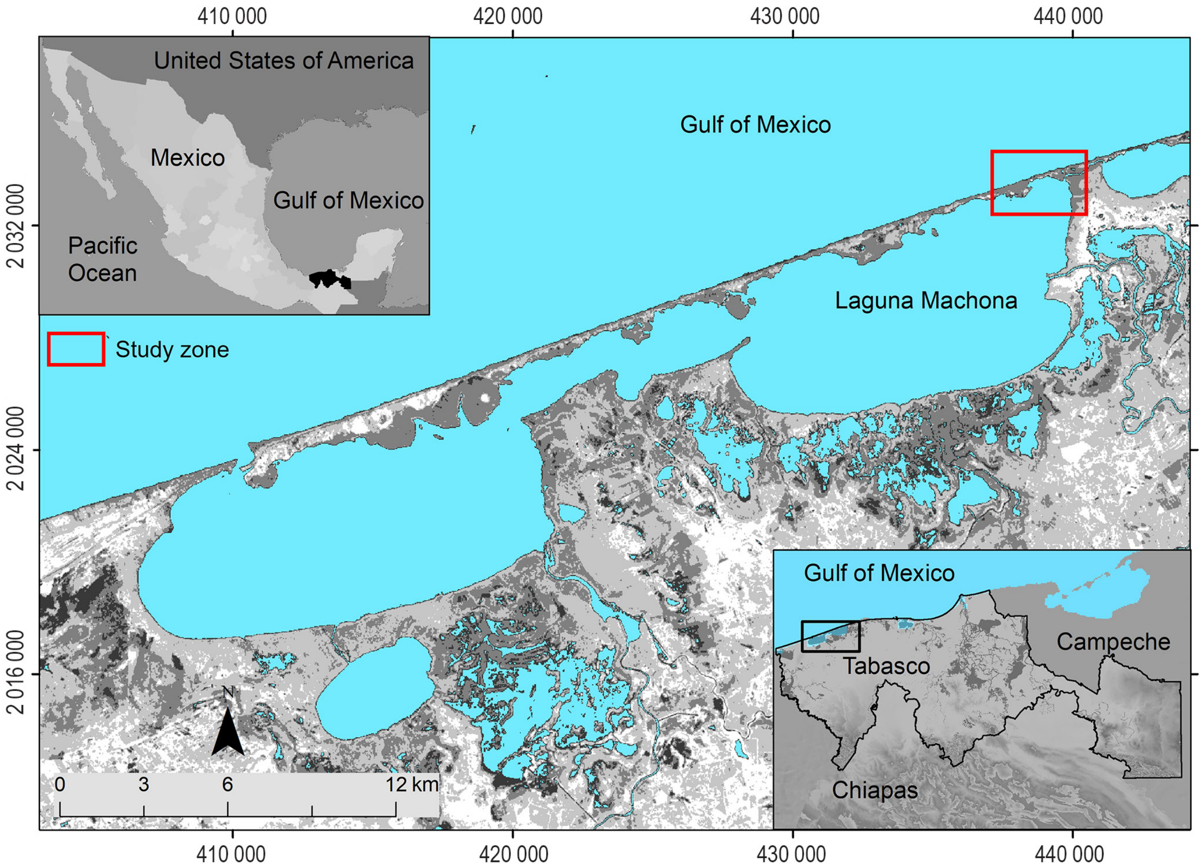

Fig. 1. Localization zone. The Carmen-Pajonal-Machona lagoon, Tabasco, Mexico (source: Authors´ own elaboration)

The red frame indicates the study zone.

face k, A_k is the area of the cell on the face k (m^2), and u is the velocity gradient in the cell ($m \cdot s^{-1}$), and two versions of the equations of motion (Brunner, 2023). One that uses the complete equations named Shallow Water Equations (SWE – Eq. 2a) written as:

$$\frac{\partial V}{\partial t} + (V \cdot \nabla)V + f_c k \times V = -g\nabla z_s + \frac{1}{h}\nabla \cdot (\nu_t h V) - \\ -\frac{\tau_b}{\rho R} + \frac{\tau_s}{\rho h} - \frac{1}{\rho}\nabla P_a \qquad (2a)$$

where V is the velocity vector in its Cartesian directions $((u,v)^T)$ ($m^2 \cdot s$), v is the turbulent viscosity tensor term ($m^2 \cdot s$), ∇ is the gradient operator, k is the unit vector of the vertical direction, τ_s is the surface wind shear vector (kg-m $\cdot$ s^{-2}), τ_b is the shear vector for the bottom (kg-m $\cdot$ s^{-2}), P_a is the atmospheric pressure (kg-m $\cdot$ s^{-2}), f_c is the Coriolis parameter ($1 \cdot s^{-1}$), z_s is the elevation of the water surface (m), R is the hydraulic radius (m), and g is the acceleration of gravity ($m \cdot s^{-1}$) (Brunner, 2023).

The other version solves the system faster because it only takes the diffusive term named the Diffusion Wave equation (DWE – Eq. 2b):

$$\frac{gn^2}{R^{4/3}} + |V|V = -g\nabla Z_s - \frac{1}{\rho}\nabla P_a + \frac{\tau_s}{\rho h} \qquad (2b)$$

The selection of SWE or DWE is a function of the addressed problem. However, since the simplified equations (DWE) are programmed by default in HEC-RAS and the complete equations (SWE) can take between three and five times more computation time, it is frequent that only the simplified ones are used. Therefore, we decided to include both results, compare them, and analyze the error generated by the simplification.

CALCULATION DOMAIN

We considered the rectangular shape geometry used as the calculation domain in the 2016 study (Ballester and Castro, 2016) as the initial condition; for comparative purposes, we will call it the original condition (Figure 2a). In addition, four computational domains were proposed: three semi-circular geometries of different sizes (Figures 2b, c y d) – emulating how the program DELFT3D works (Deltares, 2023), and one cross-section (Figure 2e).

BOUNDARY CONDITIONS

Upstream, two boundary conditions were used: a) with a flow contribution (FC) from the Santana River; and b) without flow contribution (NFC). In the first condition, the full bank discharge from the Santana River, equal to 229.02 $m^3 \cdot s^{-1}$ was applied, and in the second condition was zero. Downstream, also called open water or offshore condition (Lam et al. 2009; Provan et al. 2018), the tidal level h was proposed in both conditions. The latter was estimated from Eq. 3 (Ballester and Castro, 2016):

$$h = H \cdot sen(\omega - L \cdot t) \tag{3}$$

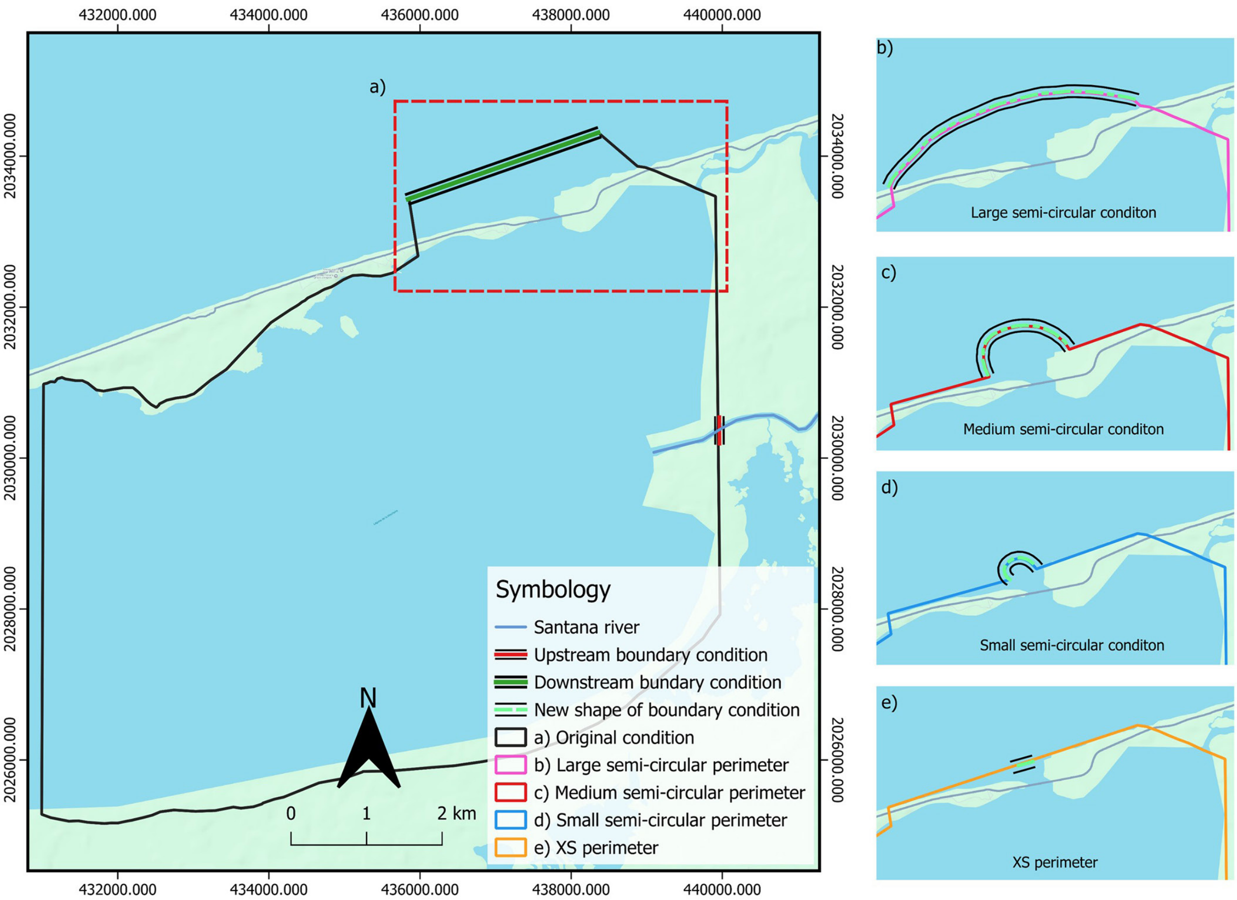

Fig. 2. Representation of the different geometric domains used in the hydrodynamic simulation (upstream and downstream): a) The original domain, b) Large semi-circular, c) Medium semi-circular, d) Small semi-circular, and e) Cross-section (source: Authors' own elaboration)

where h is the tide level (masl), H is the height of the recorded ridge or valley (m), L is the length between cycles (m), ω is the angular acceleration ($2\pi \cdot T^{-2}$) ($\mathrm{rad} \cdot \mathrm{s}^{-2}$), T is the period of oscillation (s), and t is the time interval at which we want to display the levels (s); in this case, it was one day (86 400 s).

DIGITAL ELEVATION MODEL (DEM)

The bathymetry of the lagoon bed surveyed by Ballester and Castro (2016) was used, complemented with digital elevation models from the Gulf of Mexico (INEGI, 2022). In addition, the RAS Mapper tool included in the HEC-RAS software was applied to elevate the roads and remove the breakwater built in 2016. The final bathymetry is shown in Figure 3a.

ROUGHNESS COEFFICIENT

The Manning's roughness values used in the five scenarios (Figure 3b) were estimated from the vegetation layer (INEGI, 2022), tables from the work of McCuen (1997), and reports from the United States Department of Agriculture (2022).

CALCULATION GRID

A calculation grid with 50 × 50 m cells was designed (Figure 3c); with 5 × 5 m refining zones and alignment of the cells in the direction of flow. A mesh of 59,062 cells was generated for the original condition, and 56,657 cells for the non-domain condition at sea. Alienation and refinement of the cells avoids making smaller cells throughout the domain.

SIMULATION TIME STEP

Three days were simulated with a time step of 5 seconds. Tables and graphical representations of the results were generated every 15 minutes, allowing detailed observation of variations in the system over

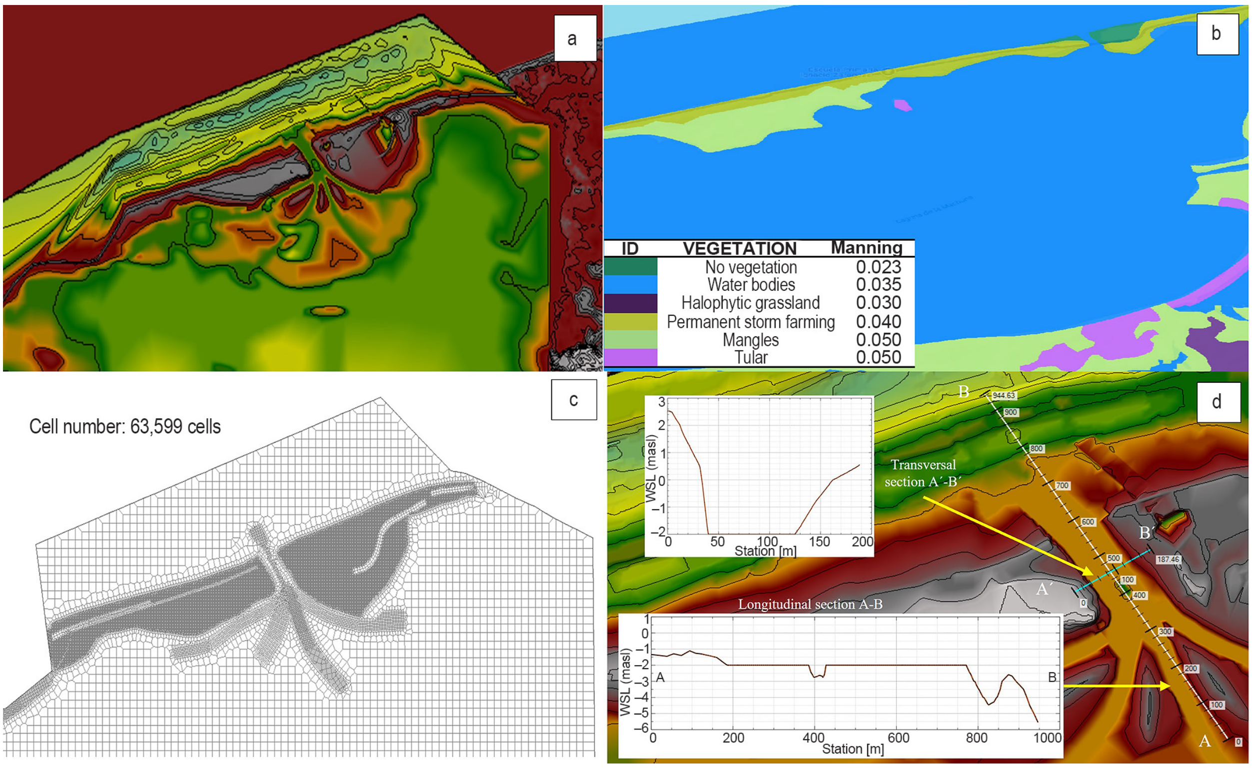

Fig. 3. Numerical conditions used: a) Bathymetry, b) Vegetation layer, c) Mesh generated, and d) Longitudinal and transverse axes used to reference the results (source: Authors' own elaboration)

time. The levels obtained for comparative purposes were referenced concerning the longitudinal axis A-B, whereas the velocity results were to the transverse axis A'-B' (Figure 3d).

CALIBRATION

The numerical model was calibrated against the results measured in the field. Two cross-sections were selected. The plain, cross-section velocities, and the water surface levels (WSL) were obtained in each cross-section (Figure 4), and subsequently used to calibrate the numerical model. The calibration parameter was Manning's coefficient, which varied between 0.003 and 0.0046 at 0.0002 intervals. One cross-section was used to calibrate the model, and another was used to validate the results. The levels and the velocity results were evaluated using the classification bySutherland et al. (2004). The author proposed the Mean Absolute Error (AMAE) to assess the quality of the simulation compared with the field measurements; the calculation is produced by Eq. (4):

$$AMAE = \frac{\langle |\underline{O} - \underline{C}| - OE \rangle}{\langle |\underline{O}| \rangle} \tag{4}$$

where $\underline{O}$ and $\underline{C}$ are the sets of observed and calculated values, respectively; OE is the observational error; and the norm $\langle\ \rangle$ is the mean absolute error. The classification is as follows: excellent $AMAE < 0.2$; good $0.2 \le AMAE < 0.4$; reasonable $0.4 \le AMAE < 0.7$; poor $0.7 \le AMAE \le 1.0$; and bad $AMAE > 1.0$. We used this classification to evaluate the calibration process.

RESULTS

Numerical model calibration

Figures 5a and 5b show the simulation results with a Manning's n of 0.032, whereas Figures 5c and 5d reflect calibration with a Manning's n of 0.040, improving the model from poor to good. Statistical methods like mean absolute and root mean square errors are helpful in manual calibrations (Butts et al., 2004; Moriasi et al., 2007). The discrepancy between measure-

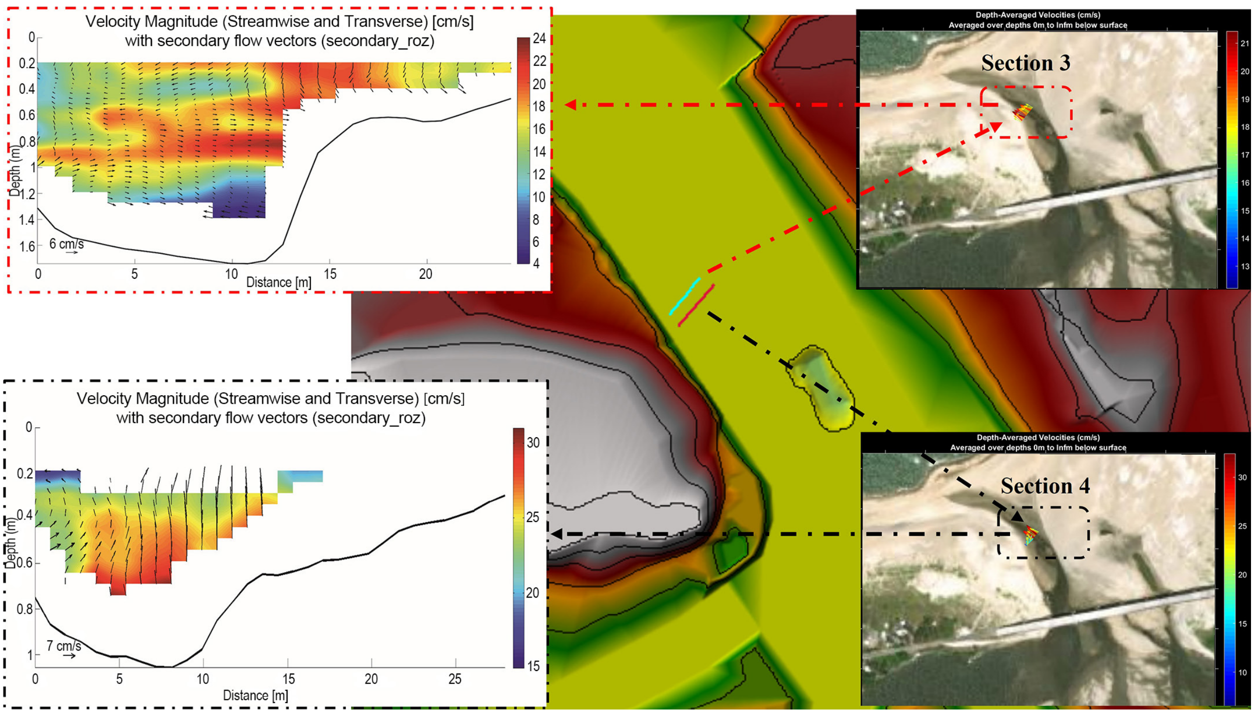

Fig. 4. Measured stations, used in the calibration and validation process (source: Authors' own elaboration)

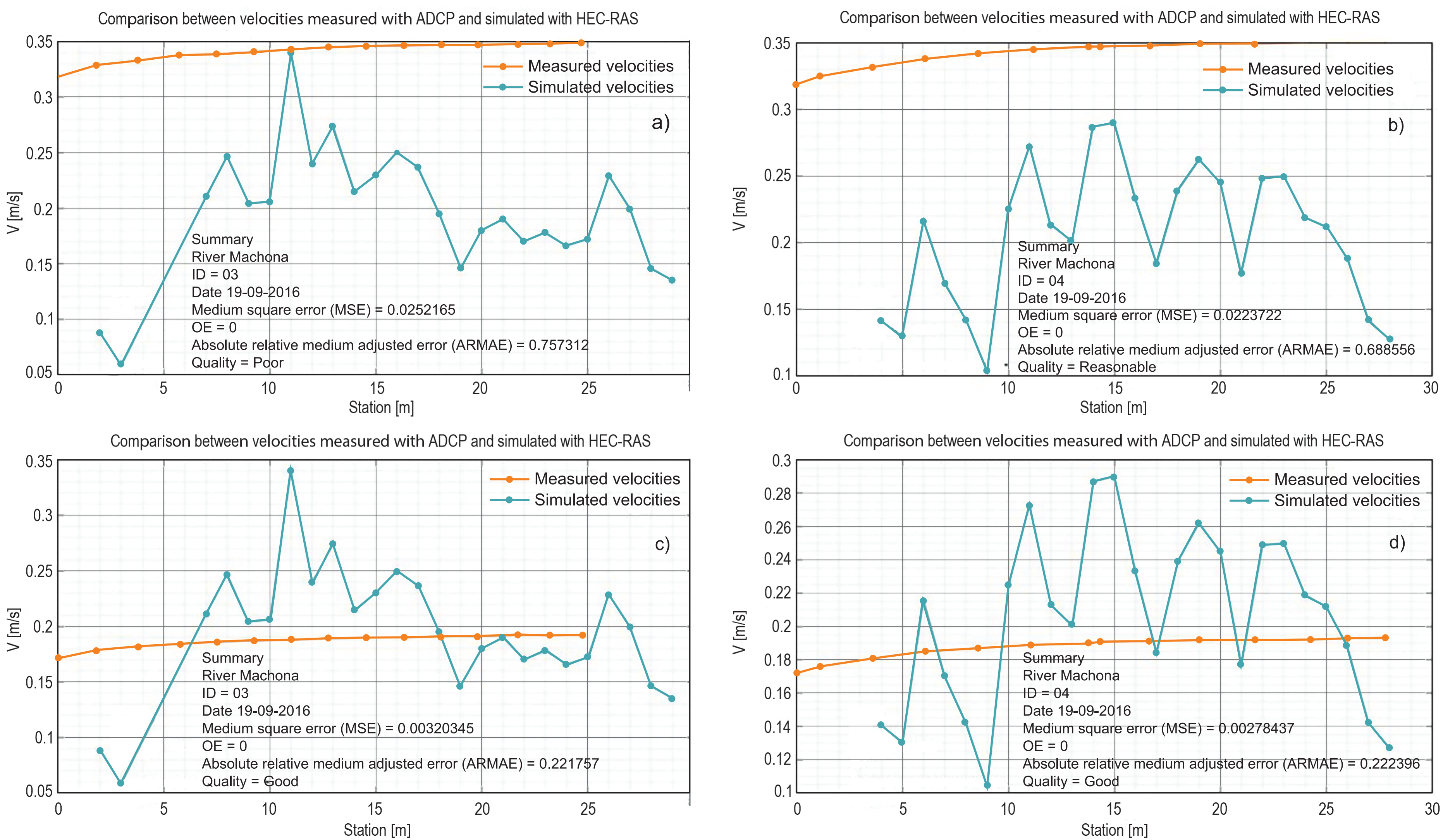

Fig. 5. Calibration process. Blue lines are the measured velocities, and red lines are the simulated ones; a) and b) are initial values for Manning n = 0.032; c) and d) are calibrated values for Manning n = 0.040 (source: Authors' own elaboration)

ments and simulations is due to the three-dimensional tidal effects, with saltwater inflow at the bottom and freshwater outflow at the surface, which a 2D model cannot fully replicate but still provides a valuable system overview.

Hydrodynamic simulation

The maximum water surface elevation (WSE) at point A along the longitudinal profile A-B was analyzed across different geometric domain configurations. Using the original domain (ORG, Figure 2a) as the reference, relative errors were calculated for configurations with and without the contribution flow (CF) from the Santana River. The analysis reveals that reducing the domain area significantly increases errors in WSE. For configurations without CF, relative errors range from 0.84% in the medium semi-circular configuration to 20.17% in the XS configuration. When CF is included, errors are substantially reduced, ranging from 0.25% to 2.47%. This stabilizing effect of CF highlights its importance in improving model accuracy, with the medium semi-circular configuration achieving the best performance in both WSE and velocity predictions.

Table 1 compares the results using the full shallow water equations (SWE) and the simplified equations (DWE). For scenarios including CF, SWE demonstrates superior accuracy, with relative errors in WSE ranging from 1% in the semi-circular configurations to 12% in the XS domain. The SWE captures inertial effects and nonlinear transitions more effectively, resulting in more accurate representations of hydraulic behavior. Conversely, the DWE exhibits significant limitations in complex flow scenarios, as shown by velocity errors of up to 66% in the XS domain. These discrepancies underscore the necessity of selecting appropriate equations based on system complexity, especially in lagoon-sea interaction studies.

Figure 6 illustrates the velocity distributions across cross-section A'-B' under various geometric domain configurations. For simulations using SWE (Figure 6a),

Table 1. Comparison of simulation results using Diffusion Water Equations (DWE) and Shallow Water Equations (SWE) under various boundary conditions (source: Authors' own elaboration)

Shape of boundary condition	Simulated condition	WSE on A (masl)			v (m · s^{-1})		
		Set Eq.		Relative error%	Set Eq.		Relative error %
		DWE	SWE		DWE	SWE	
Rectangular	NCF	0.128	0.119	7%	1.137	1.135	0.18%
	CF	0.399	0.405	2%	0.388	0.192	51%
Large semicircular	NCF	0.128	0.118	8%	1.168	1.139	2%
	CF	0.400	0.404	1%	0.406	0.195	52%
Medium semicircular	NCF	0.128	0.119	7%	1.141	1.134	1%
	CF	0.399	0.404	1%	0.376	0.192	49%
Small semicircular	NCF	0.133	0.123	8%	1.127	1.136	1%
	CF	0.400	0.405	1%	0.388	0.178	54%
XS	NCF	0.128	0.143	12%	1.212	1.224	1%
	CF	0.392	0.415	6%	0.347	0.118	66%

WSE – Water surface elevation; v – Velocity; NCF: No contribution flow; CF – Contribution flow; DWE – Diffusion water equations; SWE – Shallow water equations

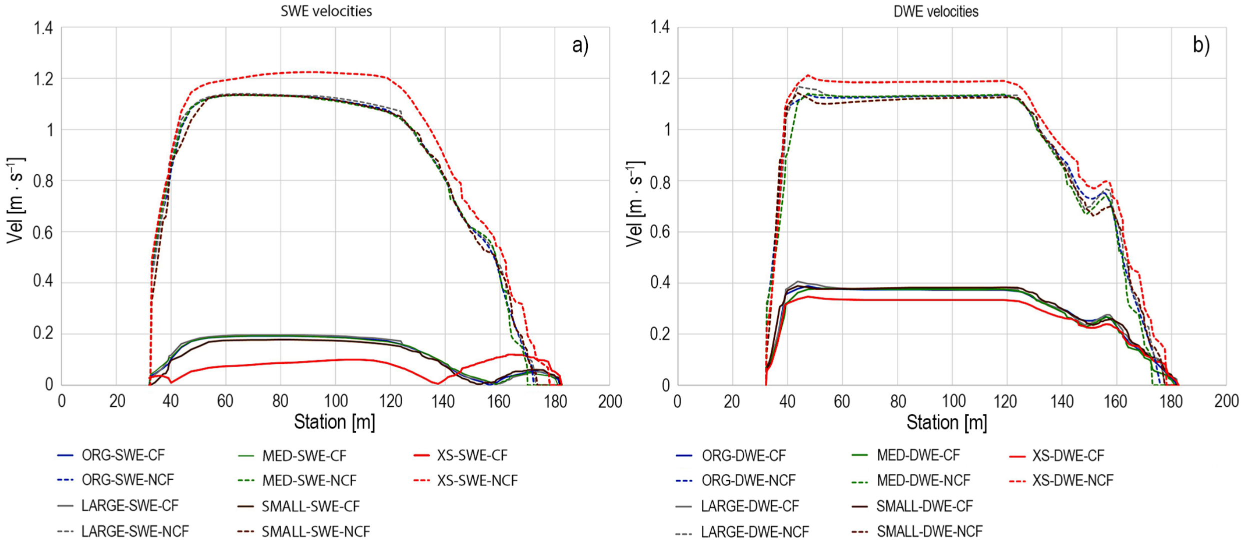

Fig. 6. Velocity distribution along the cross-section A'-B' for the different geometric domains and sets of equations; a) Shallow water equations (SWE) and b) Diffusion water equations (DWE). The simulations consider contribution flow (CF – solid lines) and no contribution flow (NCF – dashed lines) (source: Authors' own elaboration)

the MEDIUM and LARGE configurations closely replicate velocity patterns of the ORG domain, particularly near the channel's center. In contrast, the XS domain underestimates peak velocities, particularly in high-gradient areas. More significant discrepancies are observed using DWE (Figure 6b), especially near channel margins and at the center. This further confirms the superiority of SWE in capturing nuanced flow behaviors in systems with complex interactions, such as those influenced by CF.

Including CF from the Santana River significantly alters velocity magnitudes and distributions within the channel. Higher discharges increase velocities near banks and downstream areas, particularly in the XS configuration. Among the tested configurations, the MEDIUM domain balances computational efficiency and accuracy, making it the most recommended setup for modeling scenarios with CF.

Figure 7 provides a detailed comparison of water surface levels (WSL) along the longitudinal section A-B for SWE simulations with CF. The XS configuration exhibits substantial deviations from the ORG domain, particularly downstream (Figure 7b). Smaller semi-circular configurations also show discrepancies, emphasizing the critical role of domain size and shape in capturing hydraulic gradients accurately. In contrast, the MEDIUM and LARGE configurations closely match the ORG domain, offering a balance of computational efficiency and reliable representation of hydraulic gradients.

These findings highlight the importance of selecting suitable geometric domain configurations and equations for modeling estuarine systems. The MEDIUM semi-circular domain emerges as the optimal choice, especially for scenarios involving complex interactions between fluvial contributions and coastal dynamics.

DISCUSSION

This study advances the understanding of hydrodynamic modeling in estuaries by emphasizing the critical role of geometric domain configurations, specifically focusing on local-scale studies. Unlike the different scale domain compared with Ji et al. (2024), which centered on grid resolution and boundary condition sensitivity in a vast estuarine system, both studies highlight the importance of accurately capturing tidal dynamics and flow interactions. Ji et al. (2024) work demonstrated the role of wind and freshwater

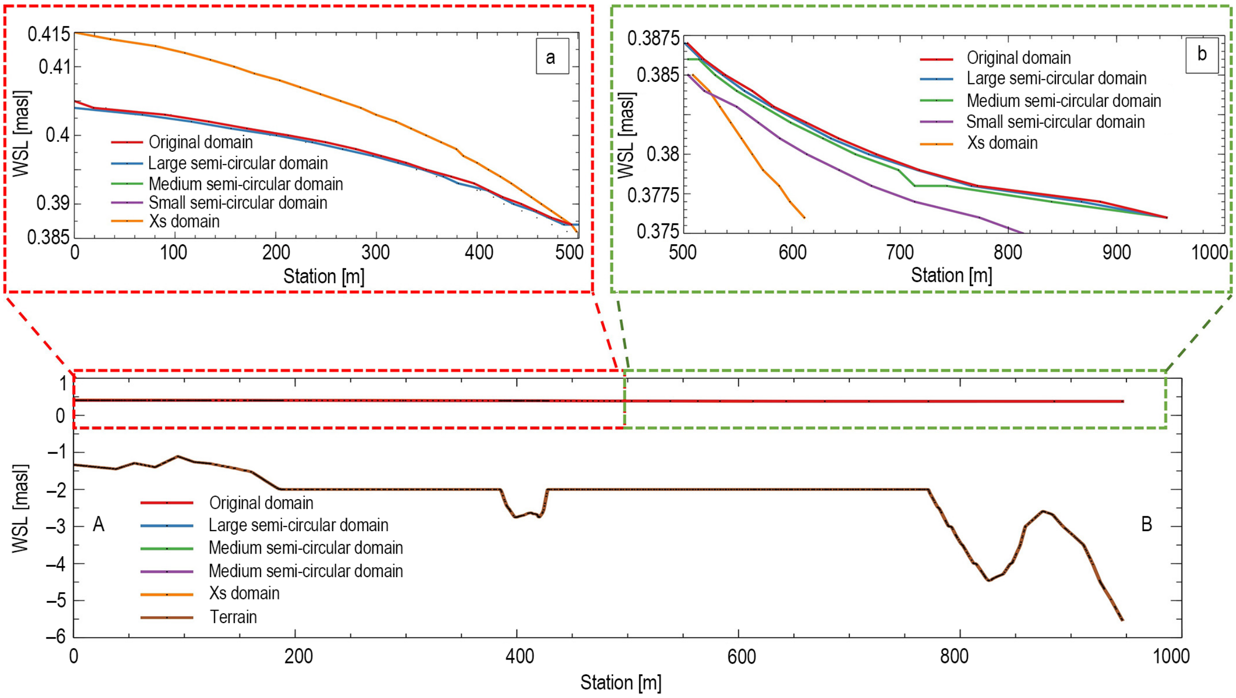

Fig. 7. Water surface elevation along the longitudinal profile A-B for the different geometric domains, SWE equations, and contribution flow from the Santana River. a) Upstream section of the longitudinal profile, and b) Downstream section (source: Authors' own elaboration)

inflows in modulating estuarine behavior, which resonates with our findings on the stabilizing effects of contribution flow (CF) from upstream sources. This parallel indicates that despite the difference in scale, the interplay between external forcings and internal domain characteristics is a consistent determinant of model performance.

The importance of local studies is reinforced by findings such as those presented by Weng et al. (2020), who used MIKE 21 to evaluate the ecological impact of sluice-gate operations in the Jiaojiang River Estuary, demonstrating that small-scale modeling can accurately predict changes in salinity and nutrient distribution. Local-scale studies have proven essential for accurate flood risk management and ecological restoration. For example, domain configurations in smaller coastal and estuarine systems significantly affect flow dynamics, sediment transport, and pollutant dispersion, requiring fine-tuned modeling approaches. Research conducted by Hein (2021) who studied tidal oscillations in semi-closed estuaries and by Sohrt et al. (2021) who analyzed tidal wave reflection in narrow estuarine channels, in their findings emphasize the need for high-resolution models that capture the intricate flow patterns within confined spaces. These local studies highlight that simplified or generalized models may miss critical processes, especially in systems where minor hydrodynamic variations can have amplified consequences, such as flood-prone urban estuaries or sensitive ecosystems. In this sense, and with these aspects in mind, our findings that semi-circular domains optimize the balance between accuracy and computational efficiency align with Sohrt et al. (2021) observation that domain geometry critically influences wave propagation and reflection. Additionally, the stabilizing role of contribution flow (CF) from upstream, demonstrated in this study, resonates with Weng et al. (2020) analysis of sluice-gate operations, where freshwater influx mitigated drastic salinity fluctuations. While these studies utilized varied numerical tools, from HEC-RAS to MIKE 21 and TELEMAC-2D, they underscore the necessity of tailoring model configurations to the studied system's spatial scale and hydrodynamic complexity.

CONCLUSIONS

This study highlights the critical importance of domain configuration, sediment characterization, and the use of full equations (SWE) in hydrodynamic modeling for river systems. The results demonstrate that accurate modeling requires careful input parameter selection, domain design selection, and applying full equations to realistically capture flow dynamics, especially under conditions with rapid and complex variations.

The analysis of water surface levels (WSL) and velocities across different geometric configurations revealed significant impact of domain shape and size on simulation outcomes. Smaller domains, such as the XS configuration, exhibited substantial deviations from the original domain, particularly in critical upstream and downstream sections. These discrepancies extended to velocity fields, where the XS domain failed to accurately capture hydraulic gradients and flow dynamics, underscoring its limitations for realistic simulations.

Having said that, medium and large semi-circular domains closely approximated the results of the original domain, providing accurate representations of WSL and velocity distributions. Among these, the medium semi-circular domain is the most suitable configuration due to its balance between computational efficiency and precision. This configuration effectively captures the hydraulic behavior of the system while requiring fewer computational resources than larger options, making it particularly advantageous for practical applications such as in flood risk assessment, infrastructure design, and river management.

Full equations (SWE) allowed for more detailed and precise simulation of flow dynamics, especially in channels connected to lagoons and under conditions with pronounced hydraulic gradients or complex flow-structure interactions. These equations represented areas of high shear stress and recirculation zones, which are fundamental for analyzing sediment transport and flow-structure interactions.

The integration of advanced remote sensing techniques, such as aerial photogrammetry and sediment size calibration, was essential for accurate input parameterization. These methodologies enhanced the resolution and precision of terrain and sediment datasets, strengthening the robustness of the model results.

Despite these advancements, the study faced some limitations, such as simplifying boundary conditions and potential errors in sediment characterization due to equipment constraints. Future research should focus on refining boundary condition definitions, exploring dynamic sediment transport processes, and validating models under diverse hydrological scenarios. Incorporating real-time monitoring data, extended use of full equations, and expanding the scope of domain geometries could further enhance the predictive capabilities of hydrodynamic models, supporting more effective decision-making in water resource management.

REFERENCES

Bakhtyar, R., Maitaria, K., Velissariou, P., Trimble, B., Mashriqui, H., Moghimi, S., Abdolali, A., Van der Westhuysen, A.J., Ma, Z., Clark, E.P., Flowers, T. (2020). A new 1D/2D coupled modeling approach for a riverine-estuarine system under storm events: Application to Delaware River Basin. Journal of Geophysical Research: Oceans, 125 (9). DOI: 10.1029/2019JC015822

Ballester, J., Castro, J.A. (2016). Diagnóstico, proyecto ejecutivo, estudio de impacto ambiental, y propuesta de actividades para la construcción de obras tipo escolleras en boca de panteones y desazolve de canales en la laguna la machona del Ejido El Alacrán municipio de Cárdenas estado de Tabasco. Diagnosis, executive project, environmental impact study, and proposed activities for the construction of jetty-type structures at the mouth of Panteones and dredging of channels in La Machona lagoon, El Alacrán ejido, municipality of Cárdenas, state of Tabasco. Tabasco, Mexico: CONAPESCA, Secretaria de Agricultura y Ganadería, Desarrollo Rural, Pesca y Alimentación. (In Spanish)

Brunner, G. (2021). HEC-RAS 2D User's Manual. https://www.hec.usace.army.mil/confluence/rasdocs/r2dum/latest (accessed: November 25, 2022).

Brunner, G. (2023). HEC-RAS Hydraulic Reference Manual. https://www.hec.usace.army.mil/confluence/rasdocs/ras1dtechref/latest (accessed: January 17, 2023).

Butts, M.B., Payne, J.T., Kristensen, M., Madsen, H. (2004). An evaluation of the impact of model structure on hydrological modelling uncertainty for streamflow simulation. Journal of Hydrology, 298 (1–4), 242–266. DOI: 10.1016/j.jhydrol.2004.03.042

Clunies, G.J., Mulligan, R.P., Mallinson, D.J., Walsh, J.P. (2017). Modeling hydrodynamics of large lagoons: Insights from the Albemarle-Pamlico Estuarine System. Estuarine, Coastal and Shelf Science, 189, 90–103. DOI: 10.1016/j.ecss.2017.03.012

de Haas, T., Pierik, H.J., van der Spek, A.J.F., Cohen, K.M., van Maanen, B., Kleinhans, M.G. (2018). Holocene evolution of tidal systems in The Netherlands: Effects of rivers, coastal boundary conditions, eco-engineering species, inherited relief and human interference. Earth-Science Reviews, 177, 139–163. DOI: 10.1016/j.earscirev.2017.10.006

Deltares (2023). Delft3D 3D/2D modelling suite for integral water solutions. https://oss.deltares.nl/web/delft3d/manuals (accessed: November 20, 2022).

Diedhiou, R., Sambou, S., Kane, S., Leye, I., Diatta, S., Sane, M.L., Ndione, D.M. (2020). Calibration of HEC-RAS model for one dimensional steady flow analysis – A case of Senegal River Estuary Downstream Diama Dam. Open Journal of Modern Hydrology, 10 (03), 45–64. DOI: 10.4236/ojmh.2020.103004

Douglass, S., Webb, B. (2020). HEC-25 – Highways in the coastal environment. 3rd Edition. https://www.fhwa.dot.gov/engineering/hydraulics/pubs/hif19059.pdf (accessed: : November 20, 2022).

Hein, S.S.V., Sohrt, V., Nehlsen, E., Strotmann, T., Fröhle, P. (2021). Tidal oscillation and resonance in semi-closed estuaries – Empirical analyses from the Elbe Estuary, North Sea. Water (Switzerland), 13 (6), 848. DOI: 10.3390/w13060848

Hernandez-Ramon, J.A., Priego-Hernandez, G., Plesiński, K.K., Rivera-Trejo, J.G.F. (2023). Management of an urban lagoon. Study case: Ilusiones Lagoon, Tabasco, Mexico. Ecosistemas y Recursos Agropecuarios, 10 (3). DOI: 10.19136/era.a10n3.3756

INEGI (2022). México en cifras. https://www.inegi.org.mx/app/areasgeograficas/#collapse-Resumen (accessed: September 25, 2022).

Ji, Z.G. (2008). Hydrodynamics and water quality modeling rivers, lakes, and estuaries. USA: John Wiley & Sons. DOI: 10.1002/9781119371946

Ji, Z.G., Moustafa, M.Z., Hamrick, J. (2024). Hydrodynamic modeling of a large, shallow estuary. Journal of Marine Science and Engineering, 12 (3), 381. DOI: 10.3390/jmse12030381

Kennish, M.J. (2002). Environmental threats and environmental future of estuaries. Environmental Conservation, 29 (1), 78–107. DOI: 10.1017/S0376892902000061

Keong, Y.C., Yusoff, M.A.M. (2022). Flood simulation using HEC-RAS for Sg Suloh, Batu Pahat. Recent Trends in Civil Engineering and Built Environment, 3 (1), 1474–1483. DOI: 10.30880/rtcebe.2022.03.01.164

Lam, N.T., Stive, M.J.F., Wang', Z.B., Verhagen, J., Thi, V., Thur, T. (2008). Hydrodynamics and morphodynamics of a seasonally forced tidal inlet system. Journal of Water Resources and Environmental Engineering, 23, 114–125.

Manina, M., Halaj, P., Jurík, L., Kaletová, T. (2020). Modelling seasonal changes of longitudinal dispersion in the Okna River. Acta Sci. Pol. Formatio Circumiectus, 19 (1), 37–46. DOI: 10.15576/ASP.FC/2020.19.1.37

McCuen, R.H. (1998). Channel geomorphology. In: P. Hall (Ed.), Hydrologic Analysis and Design. 2nd ed. Pearson Education: Prentice Hall, 130–135.

Moriasi, D.N., Arnold, J.G., Liew, M.W., Van, Bingner, R.L., Harmel, R.D., Veith, T.L. (2007). Model evaluation guidelines for systematic quantification of accuracy in watershed simulations. American Society of Agricultural and Biological Engineerings, 50 (3), 885–900.

Namara, W.G., Damisse, T.A., Tufa, F.G. (2021). Application of HEC-RAS and HEC-GeoRAS model for flood inundation mapping, the case of Awash Bello Flood Plain, Upper Awash River Basin, Oromiya Regional State, Ethiopia. Modeling Earth Systems and Environment, 8, 1449–1460. DOI: 10.1007/s40808-021-01166-9

Nizar, Y., Touazit, A., Igouzal, M. (2022). Predicting the thermal regime of the Sebou River Estuary (Morocco) using a one-dimensional model (HEC-RAS 5.0). Nature Environment and Pollution Technology, 21, 2, 883–890. DOI: 10.46488/NEPT.2022.v21i02.051

Ongdas, N., Akiyanova, F., Karakulov, Y., Muratbayeva, A., Zinabdin, N. (2020). Application of Hec-Ras (2d) for flood hazard maps generation for Yesil (Ishim) River in Kazakhstan. Water (Switzerland), 1 2(10), 1–20. DOI: 10.3390/w12102672

Peng, A., Liu, F. (2019). Flooding simulation due to Hurricane Florence in North Carolina with HEC RAS. http://arxiv.org/abs/1911.09525.pdf (accessed: September 25, 2022).

Priego-Hernández, G., Rubio-Arias, H., Rivera-Trejo, F. (2019). ADCP, Multi-frequency analysis for flow measurements in rivers. Acta Sci. Pol. Formatio Circumiectus, 18 (1), 101–112. DOI: 10.15576/ASP.FC/2019.18.1.101

Provan, M., Logan, S., Nistor, I., Cornett, A., Drouin, A. (2018). Field and numerical investigations of the morpho-hydrodynamic processes of the tidal inlet at Shippagan Gully, New Brunswick, Canada. Coastal Engineering Journal, 60 (4), 400–422. DOI: 10.1080/21664250.2018.1492235

Seabergh, W. (2008). Hydrodynamics of tidal inlets, II. Hydrologic Engineering Center. blob:resource://pdf.js/b4ceed8a-df63-461f-a0d8-67c608d72c4e#filename=EM_1110-2-1100_Ch_06.pdf (accessed: November 20, 2022).

Sedigh, M., Tomlinson, R., Cartwright, N., Etemad-Shahidi, A. (2016). Numerical modelling of the Gold Coast Seaway area hydrodynamics and littoral drift. Ocean Engineering, 121, 47–61. DOI: 10.1016/j.oceaneng.2016.05.002

Shan, X., Sun, P., Jin, X., Li, X., Dai, F. (2013). Long-term changes in fish assemblage structure in the Yellow River estuary ecosystem, China. Marine and Coastal Fisheries, 5 (1), 65–78. DOI: 10.1080/19425120.2013.768571

Sohrt, V., Hein, S.S.V., Nehlsen, E., Strotmann, T., Fröhle, P. (2021). Model based assessment of the reflection behavior of tidal waves at bathymetric changes in estuaries. Water (Switzerland), 13 (4), 489. DOI: 10.3390/w13040489

Soto-Cortes, G., Rivera-Trejo, F., Konsoer, K., Langendoen, E. (2022). HydroAPP, 2D Hydrodynamic calibration (V2; Issue August, p. 72). Mendeley Data, V2. DOI: 10.17632/549d9g469w.2

Sutherland, J., Walstra, D.J.R., Chesher, T.J., van Rijn, L.C., Southgate, H.N. (2004). Evaluation of coastal area modelling systems at an estuary mouth. Coastal Engineering, 51 (2), 119–142. DOI: 10.1016/j.coastaleng.2003.12.003

United States Department of Agriculture (2010). Time of Concentration. In: National Engineering Handbook (p. 6). https://www.hydrocad.net/neh/630ch15.pdf (accessed: December 08, 2022).

United States Department of Agriculture (2022). Hydrokinetics. In National Engineering Handbook, 24–25). https://directives.nrcs.usda.gov//sites/default/files2/1720463061/Chapter%203%20-%20Hydrokinetics.pdf (accessed: December 8, 2022).

Weng, X., Jiang, C., Zhang, M., Yuan, M., Zeng, T. (2020). Numeric study on the influence of sluice-gate operation on salinity, nutrients and organisms in the Jiaojiang River Estuary, China. Water (Switzerland), 12(7), 2026. DOI: 10.3390/w12072026

WPŁYW DOMENY GEOMETRYCZNEJ NA MODELOWANIE HYDRODYNAMICZNE NA GRANICACH ESTUARIÓW

ABSTRAKT

Cel pracy

Numeryczne modelowanie estuariów jest procesem złożonym, ze względu na działanie pływów oraz ich interakcje pomiędzy ujściem estuarium a morzem. W związku z tym pojawia się następujące pytanie: Czy długość i kształt domeny geometrycznej na dolnej granicy estuarium – a więc czy interakcja między laguną i otwartym morzem – wpływają na modelowanie hydrodynamiczne tego estuarium?

Materiał i metody

Dwuwymiarowe (2D) symulacje numeryczne przeprowadzono przy użyciu oprogramowania HEC-RAS V6.3.1. Dane wejściowe obejmowały cyfrowy model o wysokiej rozdzielczości, badanie batymetryczne badanego obszaru, dane pływowe oraz kampanię pomiarów terenowych. Przetestowano pięć typów domen geometrycznych, definiujących warunki brzegowe w dole rzeki: prostokątne; duże półkoliste; średnie półkoliste; małe półkoliste oraz przekrój poprzeczny. Dodatkowo przetestowano dwa typy wersji równań: uproszczone, uwzględniające tylko elementy dyfuzji, oraz pełne.

Wyniki i wnioski

Do analizy wyników wybrano dwa profile: podłużny i poprzeczny nad ujściem estuarium (kanał łączący lagunę z morzem). Porównano poziomy powierzchni wody, nachylenie hydrauliczne, a także prędkości. Stwierdzono niewielką istotną różnicę w odniesieniu do warunków z dominacją morza, lecz znaczną różnicę w warunkach przekroju poprzecznego. Ponadto, zgodnie z oczekiwaniami, stwierdzono istotne różnice w obliczeniach przy użyciu pełnych i uproszczonych równań.

Słowa kluczowe: HEC-RAS, warunki brzegowe, symulacja numeryczna, pomiary terenowe